THE ASTROPHYSICAL JOURNAL, 475:373–379, 1997 January 20

AN IMAGING NULLING INTERFEROMETER TO STUDY EXTRASOLAR PLANETS

J. R. P. ANGEL AND N. J. WOOLF
Steward Observatory, University of Arizona, Tucson, AZ 85721; rangel@as.arizona.edu, nwoolf@as.arizona.edu
Received 1996 May 20; accepted 1996 August 5

ABSTRACT

Interferometric techniques offer two advantages for the detection and analysis of thermal radiation from planets: destructive interference to strongly suppress the stellar emission, and the possibility of high-resolution imaging to resolve planets and distinguish them from dust emission. This paper presents a new interferometric configuration in which the conflicting requirements for these goals are reconciled. It realizes a very strong, broad interference null, so high-resolution fringes can be used while maintaining good suppression of the stellar disk. Complex phase measurement is precluded by the need for destructive interference, but we find that a cross-correlation technique analogous to aperture synthesis can recover true images. When operated 5 AU from the Sun to escape background emission from local zodiacal dust, the interferometer's sensitivity will be limited fundamentally by noise in the photon flux from warm zodiacal dust in the planetary system under observation. In order to scale the interferometer for adequate sensitivity, the 10 μm emission from such dust could be determined early on by a ground-based interferometer. If stars at 10 pc distance have zodiacal clouds like our own, a 50 m long space interferometer with four 1 m elements should see individual planets like the Earth in images taken over 10 hours. Simultaneous infrared spectra of planets like Earth, Venus, Jupiter, and Saturn could be obtained during a 3 month integration, with the sensitivity to detect carbon dioxide, water, and ozone at the levels seen in Earth's spectrum.

Subject headings: instrumentation: interferometers — planetary systems — space vehicles — techniques: image processing

1. INTRODUCTION

The past year has seen the detection of several planetary systems. Planets with masses ranging from 0.5 to 10 times the mass of Jupiter have been found at orbital radii of 0.05–2 AU around four stars at typical distances of 10–20 pc (Mayor & Queroz 1995; Marcy & Butler 1996; Latham et al. 1989). The detections so far have been with ground-based telescopes, from measurements of the reaction motion of the star they orbit. This technique is not sensitive enough to detect planets like Earth, with 1/300 the mass of Jupiter. To find these we must turn to direct images, made preferably in the thermal infrared, where the planet's emission is strongest and the star's is relatively weaker. The physical conditions on terrestrial planets, in particular atmospheric composition, would also be best studied through spectroscopy in the infrared, where absorption features are strong (Angel, Cheng, & Woolf 1986, hereafter ACW). Venus, Earth, and Mars all show carbon dioxide at 15 μm, and the Earth uniquely shows water at 7–8 μm and ozone at 9.7 μm, the latter of special interest since oxygen originates with photosynthesis (Owen 1980). Thus, we are led to the idea of a single instrument that could first detect Earth-like planets through their radiated heat, and then we undertake spectroscopic analysis in the same spectral range.

Such an instrument would have to be in space because the heat emitted by a distant planet would be swamped by radiation from the Earth's atmosphere, and from mirrors at air temperature. Even in space, completely free of atmospheric distortion as well as emission, it will still be difficult to distinguish the thermal emission of a planet against the brilliant nearby star. The contrast ratio of Sun/Earth is 10^7 at 10 μm wavelength, much more tractable than the factor 10^{10} in reflected visible light, but still very challenging. The difficulty is compounded by tiny angular separation, 0.″1 for a planet 1 AU from a star at 10 pc. A conventional, filled aperture telescope could in principle achieve the required resolution and sensitivity, but even using an optimum apodization method to suppress the diffracted star halo (ACW), a mirror diameter of 60 m would be needed, beyond the reach of present technology, though such a telescope might be required in the future to obtain high-resolution spectra of planets.

We turn to interferometric techniques that offer the possibility of high spatial resolution with small apertures, following the basic concept devised by Bracewell (1978), Bracewell & MacPhie (1979), and MacPhie & Bracewell (1979). They envisaged detecting planets in the infrared by combining out of phase the light from two small apertures $\sim$20 m apart, so as to cancel the stellar flux over a broad wave band. Any residual uncancelled radiation of the star together with the signal of the planet occur together in the Airy disk. Given a suitable baseline, a close planet's emission will reinforce (constructive interference), while the disk of the star is suppressed. An interferometer of length $2s$ and orientation θ yields Young's fringes with amplitude a and transmitted intensity T given by

$$a = \sin \phi \ , \quad T = a^2 = \sin^2 \phi \ , \tag{1}$$

where

$$\phi = (2\pi\alpha s/\lambda) \cos (\beta - \theta) \tag{2}$$

Here the source is an element at angular separation α from the median plane of the interferometer and position angle β. We have neglected the fall in intensity due to the beam profile of a single aperture.

While a two-element interferometer could be used to search for a planet like Jupiter, as envisaged by Bracewell, there is a fundamental difficulty for detecting and analyzing planets as close to a star as the Earth. This arises because

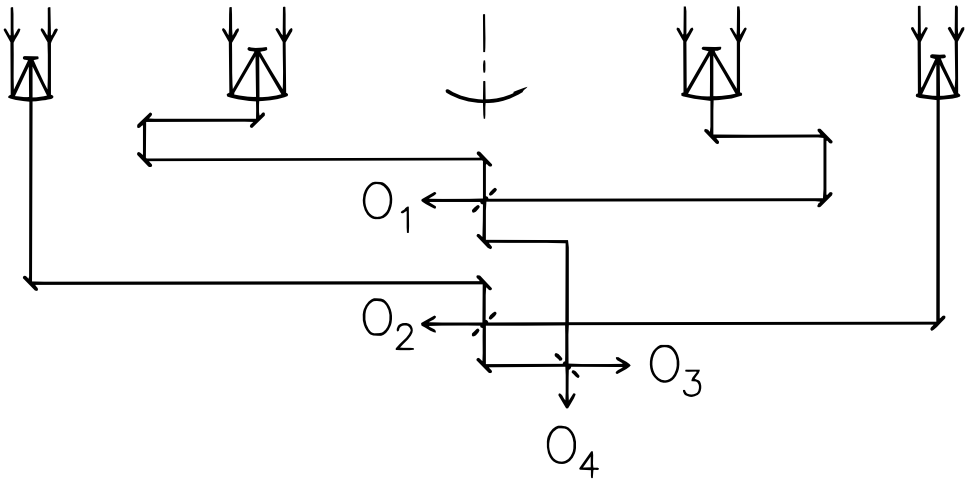

FIG. 1.—Schematic diagram of the four-element linear nulling interferometer. The fixed beam combining geometry is configured to give equal path lengths from all four telescopes. The inner and outer pairs are combined with beam splitters having equal transmitted and reflected intensities. The final combiner transmission is chosen to yield amplitudes in the ratio (inner pair/outer pair) = 0.504.

good star suppression requires a small interferometer baseline, to achieve very low transmission across the whole stellar disk, several milliarcseconds across for the nearest stars. But a small baseline does not allow full constructive interference of a close planet, or for planets to be resolved from each other or from a dust cloud in the external system. Confusion of dust with planets could especially be a problem: the solar system, for reference, emits 10 μm flux some 300 times stronger than the Earth, from about the same orbital distance.

2. A LINEAR NULLING INTERFEROMETER

We describe here a new arrangement of four elements in line, capable of realizing a uniquely broad and deep central null, together with high-resolution fringes that can be used for mapping. Signals from this interferometer can be used to reconstruct images to distinguish multiple close planets against diffuse dust cloud emission, as we show in the following section.

The very deep interference null is achieved by combining two superposed Bracewell interferometers with different spacings, whose outputs are combined with 180° achromatic phase difference (Fig. 1). The final beam-combiner ratio is chosen so that the amplitude from the outer pair is almost exactly half that from the inner pair. Then the responses of the inner and outer pair pass through zero on the median plane with equal and opposite slope, canceling to high order (Fig. 2). For spacings $2s$ and $4s$, amplitude and transmitted intensity now become

$$a = \sin\phi - \tfrac{1}{2}\sin 2\phi = 2\sin\phi\,\sin^2(\phi/2)\,, \qquad (3)$$

$$T(\alpha, \beta, \lambda, \theta) = a^2 = 4\sin^2\phi\,\sin^4(\phi/2) \sim \alpha^6/4 \text{ for small } \phi\,, \qquad (4)$$

Here ϕ is given by equation (2). Notice the dependence of intensity on α^6 near the axis, a result that gives an exceptionally broad central minimum. In practice, the amplitude of the sin 2ϕ component may be increased slightly from 0.5 to 0.504, so as to broaden further the deep minimum. Figure 2*b* shows the transmission in linear and logarithmic scales of a four-element interferometer compared to a two-element interferometer $\frac{3}{8}$ as long. We see that the added elements achieve both a much deeper and broader minimum, and narrower fringes, which will help to discriminate diffuse dust and unresolved planets. The fringe maxima are in pairs, at $\phi = 2\pi/3,\ 4\pi/3,\ 8\pi/3,\ 10\pi/3$, etc. The absolute

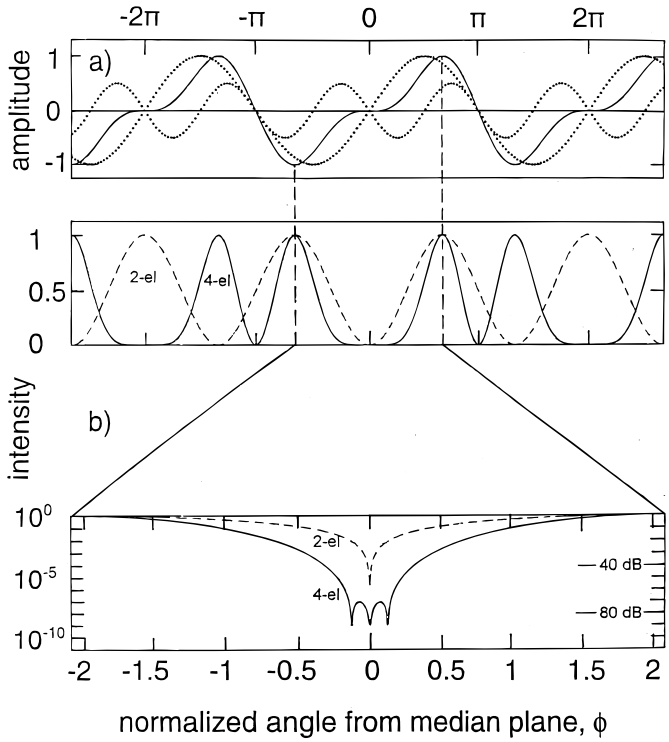

FIG. 2.—(*a*) Dotted curves show separately the fringe amplitudes for the inner and outer Bracewell pairs of the four-element interferometer (the two terms of eq. [3]). For a source at the meridian plane, both amplitudes are zero, and the slopes are equal and opposite, leading to a summed amplitude with the zeroth-, first-, and second-order terms all zero (*solid curve*). (*b*) The transmitted intensities of the four-element interferometer and of a single Bracewell pair $\frac{3}{8}$ as long, chosen to have its first maxima at the same absolute angle from the meridian plane (*broken line*). The normalized angle (which depends on length) is appropriate for the four-element interferometer. The central nulls are shown expanded and in logarithmic scale, to illustrate the much greater depth and width achieved by the four-element configuration.

transmission depends on the ratio of inner to outer pair mirror areas and reaches a maximum of 75% when this ratio is 2. In this case, a final beam combiner with $\frac{1}{3}$ transmission, $\frac{2}{3}$ reflection is required to balance amplitudes.

It is envisaged that the telescopes and beam combiner elements would be held fixed in the geometry of Figure 1 by attachment to a rigid beam held normal to the line of sight to the star under study. The path lengths leading to the final combination of the inner and outer interferometer pairs will be equalized by fixed trombone delay elements incorporated in the inner pair, as shown. Only a small range of adjustment of the mirrors would be needed to correct for structural deformation and mispointing.

For mapping purposes, the interferometer would be rotated about the line of sight like an airplane propeller, so as to cause a modulation of the flux detected from a source element at position (α, β), as in equations (2) and (4). To reveal dependence on wavelength, the infrared continuum would be dispersed and then detected in a number of separate narrow-band channels. Figure 3 shows examples of the amplitudes and intensities T that correspond to source elements with different maximum values of ϕ and position angles β.

3. IMAGE RECONSTRUCTION

Image reconstruction from signals obtained with a rotating interferometer is well known in the field of radio interferometry. Our situation is different in that the full information needed to recover surface brightness at each point (α, β) on the sky by a complex Fourier transform is not available. The radio case is illustrated by the imaging of the north polar region obtained by Ryle & Neville (1962) from an interferometer with two small elements. In this case, the rotation about the line of sight was provided by the Earth. Observations were made at a single wavelength and with many different spacings of the two elements. Phase and intensity of the detected signal were obtained from detectors in phase quadrature.

In our case, rotation gives all position angles, which is only possible in radio astronomy for circumpolar objects. Changes in element spacing are inadvisable because of the risk of mechanical failure. But for continuum sources, the signals obtained at different wavelengths are equivalent to those from different baselines at the same wavelength. The possibility of using this equivalence in radio interferometers has been discussed (Thompson 1962) but is rarely used in practice. The main difference for the nulling interferometer is that signal phases in quadrature cannot be determined, since only the phase combination that nulls the stellar emission is useful.

Despite the lack of complex phase, images can be recovered by a cross-correlation method analogous to the radio Fourier transform. Thus,

$$I(\alpha, \beta) = \sum_{\lambda} \sum_{\omega} D(\lambda, \theta) T(\alpha, \beta, \lambda, \theta) . \quad (5)$$

Here $I(\alpha, \beta)$ is the surface brightness at (α, β), $D(\lambda, \theta)$ is the measured signal strength at wavelength λ and at interferometer orientation θ, and $T(\alpha, \beta, \lambda, \theta)$ is the transmission of the interferometer given by equations (2) and (4). The summation is taken over rotation angle and wavelength, and in the absence of any phase information the quantities are real, not complex. The consequence of signals that are completely symmetric about a 180° rotation of the interferometer is that each point source appears twice, reflected through the central star. However, the recovered images are otherwise of good quality, as we show below. Since developing this method, we found that the possibility for analyzing data from a nulling interferometer by cross-correlation was suggested in an unpublished paper by MacPhie & Bracewell (1978).

To obtain spectra of planetary companions, we envisage observations extended over long periods. These will be co-added to recover less noisy records in each wavelength band. Given the known positions of the planets, a least-

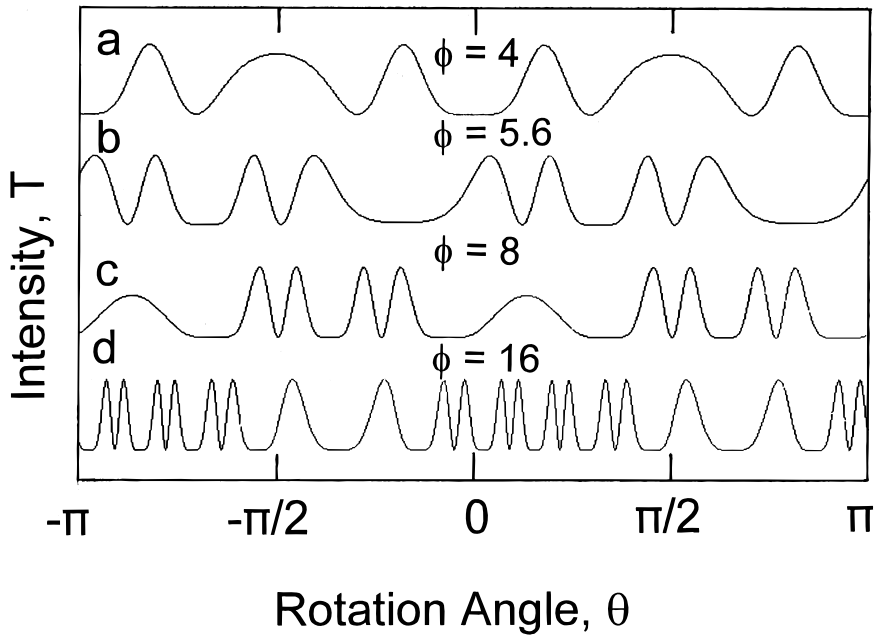

FIG. 3.—Transmitted intensities as a function of rotation angle θ for different maximum values of ϕ and position angle β

squares fitting would be used to determine for each band the individual planet fluxes that best reproduce the measured $D(\lambda, \theta)$.

4. PERFORMANCE OF A 50 m INTERFEROMETER WITH 1 m ELEMENTS

We have analyzed a design suitable for detecting and studying planetary systems around the 20 or 30 single solar-type stars within 10 pc distance. The image reconstruction technique described above has been simulated, including the effects of photon noise, to see what imaging sensitivity and spectrum accuracy should be achieved. Our model system is assumed to be at the maximum distance of 10 pc, and it includes four planets each of which emits the same strength of radiation as the Earth, and with the separations and position angles shown in Figure 4.

The interferometer consists of four 1 m mirrors with total length $4s = 50$ m. From Figure 2 we find that the central null has transmission less than $<10^{-7}$ over an angle of 3 mas, even at the shortest wavelength envisaged (6 μm). This is broad enough to reduce the stellar flux to a level comparable to or less than that of an Earth-like planet for any of the nearby stars except α Cen. At the same time, the baseline is long enough to give high-resolution fringes, with maxima at 10 μm wavelength of 0".055, 0".11, etc. An Earth-like planet 1 AU from a star at 10 pc (0".1 maximum extension) coincides with the second fringe peak, and thus it will pass through four interference maxima as the interferometer is rotated. The individual planet signals at 10 μm wavelength will vary with rotation angle as shown in Figures 3*a*–3*d*. The dependence on wavelength is such that Figure 3*b* will give a signal like that of Figure 3*a* at 14 μm and that of Figure 3*c* at 7 μm. In the absence of noise, the detected 10 μm signal from all four planets would be as in Figure 5*a*.

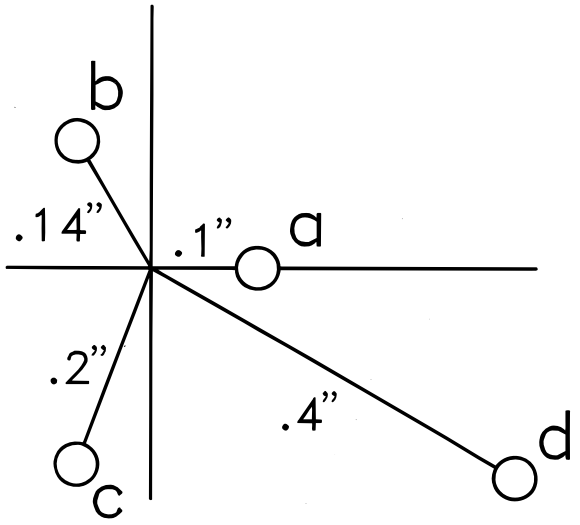

FIG. 4.—Locations of planets used to model interferometer response. Separations are given in units of arcseconds and correspond to projected separations 1–4 AU from a star seen from 10 pc.

The structured planet signals are distinct from the stronger but smooth modulation expected from an elliptical dust cloud around the star. The dependence on angle was not modeled explicitly, but such a cloud will yield a strong modulation at twice the interferometer rotation frequency. In our analysis of the simulated data, the component of modulation at the frequency is subtracted out.

To calculate photon noise levels, we assume that the background from local zodiacal dust has been reduced to a negligible level by operating the interferometer several AU from the Sun (Bracewell 1978; Leger et al. 1995). We have assumed further that other sources of noise, such as detector read noise and dark leakage, can be made negligible. The

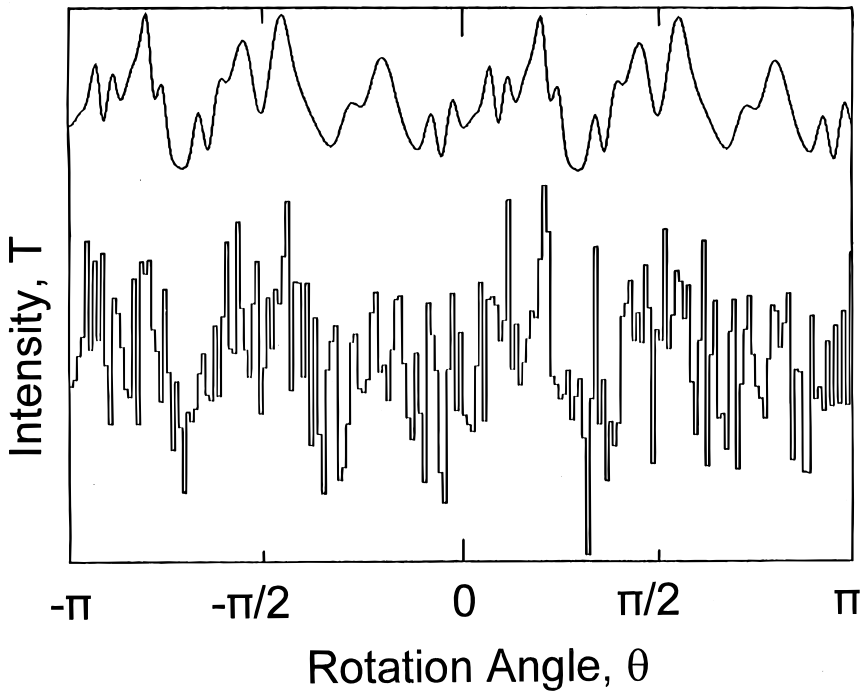

FIG. 5.—(*a*) The combined 10 μm signal for all four planets in Fig. 4. (*b*) The same signal as with the addition photon noise, as projected for a 10 hr integration and 1 μm bandwidth. Each planet is projected to be as bright as the Earth seen from 10 pc. The photon noise level is appropriate for a stellar zodiacal cloud having the same luminosity as the Sun's.

only significant source of noise is then from the star's zodiacal dust cloud, assumed to have the same temperature and density profile as found in the solar system, as deduced from *IRAS* data. The detected flux was estimated by convolving the cloud model viewed from 10 pc with the interferometer response $T(\alpha, \beta, \lambda, \theta)$. Because of the broad central null, the brightest emission, within 0.3 AU, is very strongly suppressed. The actual detected photon counts, $D(\lambda, \theta)$, for planets and cloud combined were estimated assuming 20% effective quantum efficiency for the detector and optics combined.

Under these assumptions, the time-averaged signal detected from the Earth-like planet is 0.05 photoelectrons s^{-1} in a 1 μm wide channel, and the average flux from the zodiacal cloud is 10 e- s^{-1}, some 200 times stronger. In our simulation of data taken over 10 hours, we have binned counts into 180 bins corresponding to 2° intervals in interferometer rotation angle θ and have added Gaussian noise appropriate to the cloud background count, as shown in Figure 5*b*. Similar data were simulated for all 10 bands spanning 7–17 μm,.

These data sets were used to reconstruct an image by the method of equation (5). The image shown in Figure 6 (Plate 26) is a color coded plot of intensity I_n, normalized at each radius α:

$$I_n(\alpha, \beta) = I(\alpha, \beta) - \int_0^{2\pi} I(\alpha, \beta) d\beta \, . \qquad (6)$$

It shows clearly the four planets positioned correctly with resolution (FWHM) of about 0.″02. The signal-to-noise ratio for this polychromatic 10 hour image is approximately 7, in good agreement with a projection of 10 made simply on the basis of total photon counts in the individual planet signal (17,000) and cloud background (3,400,000). As expected, the images are doubled by mirroring through the central star position. We find by trying different planet separations that the effect of subtraction of the 2ω component (done to all the synthesized data to remove cloud background) is to prevent detection of planets within $\sim 0.''1$. Such planets may become apparent when observations are extended over months, when their orbital motion should show changes distinguishable from the unchanging zodiacal cloud signal.

Based on the signal-to-noise ratio obtained for image recovery, we have estimated the integration time needed for spectroscopy. The highest signal-to-noise ratio is needed to detect ozone at the level seen in the Earth's spectrum. Allowing for an average taken over all latitudes, its equivalent width is about 0.12 μm; thus, a spectrum at a signal-to-noise ratio of 20 with resolving power 20 would be needed to make a detection at the 5 σ level. This will require a total integration some 200 times longer than for the image, about 12 weeks. The resulting quality is illustrated in Figure 7, a spectrum of the Earth shown at this signal-to-noise ratio and resolution. All three features of water, ozone, and carbon dioxide show unambiguously. In fact, carbon dioxide is so strong that an integration of a couple of weeks would be enough to show it clearly.

The long integrations required for spectroscopy will alow for deep imaging of smaller planets, and also for removal of the 180° ambiguity in position angle. Slight precession of the spin axis about the invariant axis of angular momentum, or slight deviations from the exact phase for nulling, will break the 180° symmetry, allowing full deconvolution with high signal-to-noise ratio data.

5. GROUND-BASED MEASUREMENT OF ZODIACAL CLOUD STRENGTH

It is possible that our best nearby star candidates may have dust clouds emitting more strongly at 10 μm than our own zodiacal cloud. If so, a space interferometer with larger elements will be needed to avoid excessively long integration times. For a given planet emission, the added photon noise from a 10 times brighter cloud would argue for elements 10 times the area (3.3 m diameter), otherwise 10 times longer integrations would be needed for the same signal-to-noise ratio. But such brighter clouds should be detectable with an optimized, ground-based Bracewell interferometer (Woolf & Angel 1995, p. 44) with similar resolution to the space interferometer.

Atmospheric wave front aberration that would normally prevent accurate cancellation of the stellar flux can be cor-

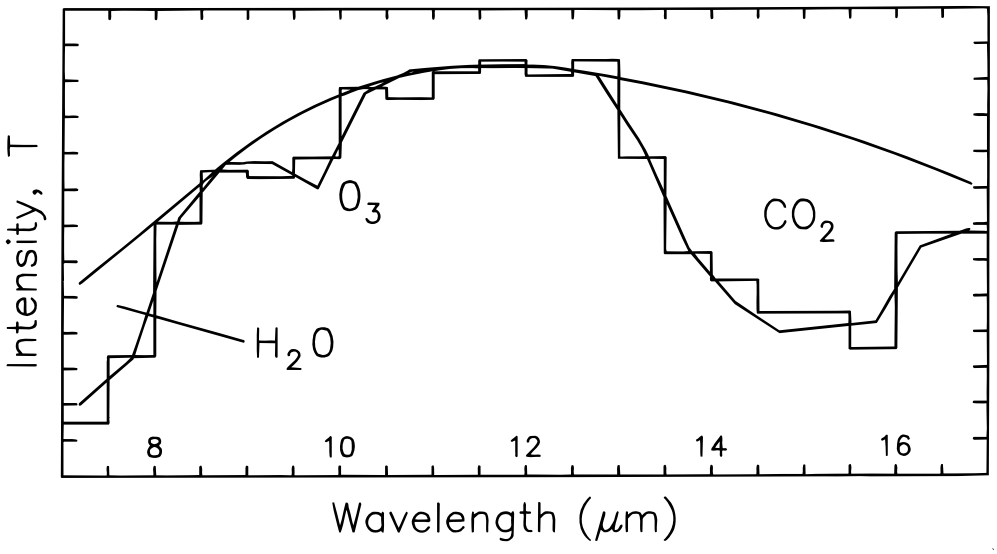

FIG. 7.—A spectrum of the Earth at a resolution of 0.5 μm and a signal-to-noise ratio of 20:1, as would be obtained from 80 days of observation of a solar system–like set of planets at 10 pc. The segmented line gives the true spectrum. The smooth line shows a blackbody curve.

rected with adaptive optics. This correction should be made at the secondary mirror (Bruns et al. 1995, p. 118), for then a high Strehl correction (>99%) should be realizable without increasing telescope emissivity above the best achieved levels of a few percent. Even so, the thermal background will be about 10^8 times brighter than at 5 AU, but on the ground large apertures can be brought to bear to reduce the beam width and photon noise. The Large Binocular Telescope (Hill & Salinari 1994), being built with two 8.4 m primaries on a common mount, will be well suited to this task. Its thermal background will be minimal because of its simple, direct beam combination and its planned use of adaptive secondaries and cooled mirrors to combine the beams. Its large element size, 8.4 m, will result in high sensitivity, and its center-to-center spacing of 14 m will provide an optimum combination of strong stellar suppression with good cloud transmission. At 10 μm wavelength, the first bright fringe peaks 0".07 from the nulled star, or 0.7 AU at a distance of 10 pc. Both the luminosity and departures from circularity of the cloud could be measured.

The integration required to overcome photon noise may be estimated in the same way as for the space interferometer. The 10 μm flux from a G2 star at 10 pc is $\sim$2 Jy, and a zodiacal cloud 3 times brighter than the Sun's would be 0.2 mJy. Interferometric cancellation of the star to below the cloud level should be achieved, given the adaptive wave front correction. The background photon flux in the individual 8.4 m diffraction-limited beams corresponds to a source of 33 Jy, with corresponding photon noise of about 2.3 mJy $Hz^{-1/2}$. Experience shows that detection at close to the photon noise level is possible by rapid chopping from source to sky. In this mode, we expect a 0.2 mJy zodiacal cloud to be detectable at the 3 σ level in about 1 hour of integration.

6. COMPARISON WITH EARLIER CONCEPTS

Our method for planet detection by imaging is distinct from earlier concepts, which rely on frequency analysis of the detected signal. With Bracewell's original two-element interferometer, a planet would be identified as a modulation at twice the rotation frequency, ω. In the first interferometer concept aimed at Earth-like planet detection, Angel (1990) described a configuration of four elements in a cross or diamond. In this case, the modulation caused by planetary companions would contain also a strong component at 4ω. The advantage was an improved null, with transmission near the null varying as α^4. Both geometries suffer the same difficulty: signals from planets close to the star would be mimicked by an elliptical dust cloud. In the concept by Leger et al., this ambiguity is overcome by an interferometer with odd symmetry, five elements distributed symmetrically around a circle. With suitable phase relations in the beam combination, the central null is again as α^4. In this case the symmetry results in five peaks around the null, and signal modulation for a planet close to the star has a strong 5ω component, as opposed to the lowest frequency of 10ω for a symmetric dust cloud. But though a planet signal is thus rendered distinct, multiple planets would be confused. Increased baseline for higher resolution fringes, which in our design allows unique deconvolution of radius and angle, is not practical in these earlier concepts. With the null varying only as α^4, the larger star disks cannot remain suppressed with baselines as large as 50 m, whereas 50 m or longer baselines could be used for the linear array, to reach beyond 10 pc or to resolve a patchy zodiacal cloud. Further, the spotty nature and regular pattern of the two-dimensional interference peaks present difficulties in achieving uniform spectral sensitivity.

The approach to suppression of local zodiacal sky background in Angel's four-element design was to use large individual elements, 8 m diameter. This results in good sensitivity, even when operated at 1 AU from the Sun. The strong signals and small beam width afforded by large elements compensate for strong zodiacal sky emission. Such large elements in local orbit might still become the favored solution, if the dust clouds of other systems are relatively strong. But in an important step, Leger et al. realized that if the solar system's cloud is typical, an interferometer operated far from the Sun would have adequate sensitivity and be much preferred in terms of economic feasibility. When both the local and stellar dust signals are low, much smaller and less expensive elements ($\sim$1 m) are sufficient.

7. PRACTICAL ASPECTS

Our focus so far has been to establish the feasibility of finding and studying Earth-like planets, within the fundamental constraints set by diffraction and photon noise and without the need for large, expensive telescope elements. But even though moderate size telescopes should be sufficient, the nulling interferometer presents many technical challenges. While a full discussion is beyond our present scope, we consider here the key issues.

1. *Wave front quality.*—As a baseline concept for the interferometer elements, we take the SIRTF (Werner & Fanson 1995), an infrared telescope with a 0.8 m beryllium mirror to be placed in solar orbit trailing the Earth. The telescope will be cooled initially by passive means to 50 K. SIRTF needs to satisfy the normal criterion for diffraction limit, so its wave front errors can be 100 times larger than our desired limit of 0.001 rad. But simple techniques could give the improvement needed. First we note that errors on a small spatial scale, such as orange peel or microroughness, should be of little consequence for our purpose. Consider a relatively large orange peel roughness of 10 nm rms on a scale of 2 mm, as might be produced when errors from 10 mirror reflections before the detector are compounded. From the Marechal approximation (e.g., Beckers 1993) we find that 2×10^{-5} of the star's 10 μm flux will be scattered as a broad halo $\frac{1}{4}$ degree in diameter, with very low brightness and negligible phase errors within the diffraction-limited beam. Low-frequency errors are potentially more troublesome, but a SIRTF quality wave front could be improved sharply without changing the telescope optics, by a spatial filter in the focal plane. Since the planetary systems to be studied lie within the single-element diffraction-limited star image, the planetary component would not be lost. Either a hole of width $\sim\lambda/d$ or a single mode fiber (Shao & Colavita 1992; Mariotti et al. 1995) could serve as the filter. The Strehl ratio entering the filter would already be >99%, so the loss in this process is little more than the $\sim$30% for filtering a perfect Airy pattern, depending on coupling details. Good fibers for transmission at up to 17 μm need still to be developed, but since the length required to suppress unwanted modes is only a few cm, materials with negligible absorption are already available.

2. *Control of phase and path length errors.*—The technique of long baseline stellar interferometry is being devel-

oped at a number of ground-based facilities now in operation. Baselines are up to 100 m and are being stabilized to accuracies of a few nm against the large rapid changes imposed by atmospheric turbulence and Earth rotation. Typically fringe phases measured at shorter wavelengths are used in a servo to control path length for observations at a longer wavelength, as we would expect also for the space interferometer. Many of the required features of optical aperture synthesis have been proven by Baldwin et al. (1996) in their interferometer yielding maps of Capella, and showing the orbital motion of the binary system. The first optical interferometer in space, the planned *Space Interferometry Mission* (*SIM*) will test further much of the required technology (Shao 1996). The length and rigidity of the nulling interferometer will go beyond the requirements for *SIM* and other space science missions, but the experience in assembling and deploying even larger structures will be gained in building the space station. The station itself could be used as a base to assemble and test the interferometer, before gentle propulsion to a distant solar orbit. Solar electric motors suitable for this are now being developed.

3. *Key technology areas specific to the nulling interferometer.*—A key step will be the experimental demonstration of beam combination of broadband infrared radiation to yield very strong destructive nulling. Concepts for achromatic phase control by reflection (Shao & Colavita 1992) and by balanced dispersive materials (Angel, Burge, & Woolf 1996) are being explored. These need to be demonstrated together with good control of amplitude and polarization, equally important in getting a very deep null. Spatial filters, including fibers, need to be developed and tested. The possibility that X-junctions in the fiber optics may be useable as high efficiency beam splitters needs to be explored.

Because the planet signal is so feeble, 22nd magnitude at N band, preservation of optical efficiency and detector efficiency is crucial. Any reduction on the assumed overall efficiency of 20% at 10 μm would need to be made up by increasing the mirror sizes. Strategies for efficient spatial filtering, spectroscopic band separation, and dielectric coatings all need to be explored over the 6–17 μm range. Infrared detectors with the required low noise characteristics (1 electron s^{-1} dark leak and 1 e- rms read noise) do not yet exist, but there are promising avenues to reach these goals (Moseley 1995).

8. CONCLUSIONS

Summarizing, the special significance of the imaging interferometer concept is as follows:

1. It exploits a new linear configuration with a deeper and broader minimum than for previously studied configurations. This allows the use of long baseline with high-resolution fringes.
2. True images of planetary systems may be reconstructed from the interferometer signals obtained by rotating the interferometer and by measuring modulation separately in multiple wavelength bands.
3. Thermal emission from planets is distinguished from that of an associated zodiacal dust cloud by virtue of the high spatial resolution, which results in complex modulation only by planets. Our illustration was a 50 m interferometer, but baselines >100 m could provide higher resolution while still strongly suppressing all but the few nearest stars. The added resolution would allow imaging of planets very close in and guard against cloud irregularities appearing as spurious planets.
4. Linear fringes, characteristic of the one-dimensional array, allow spectroscopy with uniform spectral response with no need to change array geometry. One fixed configuration is ideally suited to both the detection and spectroscopy of terrestrial planets.

This work was stimulated by NASA's initiative in 1995 to develop a road map for the study of exo-planets. We are grateful especially to Ron Bracewell for a critical reading of an earlier manuscript, to Alain Leger, Jean-Marie Mariotti, and Mike Shao for valuable discussions, Marks Sykes for solar zodiacal cloud data, and James P. Angel and Martin Woolf for their help in analysis and programming. This work is supported by the Air Force Office of Scientific Research (F49620-1-0437), NSF (AST 92-03336), and NASA (NAS 7-1260).

REFERENCES

Angel, J. R. P. 1990, in The Next Generation Space Telescope, ed. P. Bely & C. J. Burrows (Baltimore: Space Telescope Science Institute), 81
Angel, J. R. P., Burge, J., & Woolf, N. 1996, Proc. SPIE, in press
Angel, J. R. P., Cheng, A. Y. S., & Woolf, N. J. 1986, Nature, 322, 341 (ACW)
Baldwin, J. E., et al. 1996, A&A, 306, L13
Beckers, J. M. 1993, ARA&A, 31, 13
Bracewell, R. N. 1978, Nature, 274, 780
Bracewell, R. N., & Macphie, R. H. 1979, Icarus, 38, 136
Bruns, D. G., et al. 1995, in OSA Technical Digest Series 23, Adaptive Optics (Washington, DC: Optical Society of America)
Hill, J. M., & Salinari, P. 1994, Proc. SPIE, 2199, 64
Latham, D. W., Mazeh, T., Stefanik, R. P., Mayor, M., & Burki, G. 1989, Nature, 339, 38
Leger, A., Mariotti, J.-M., Mennesson, B., Ollivier, M., Puget, J. L., Rouan, D., & Schneider, J. 1995, preprint
Macphie, R. H., & Bracewell, R. N. 1978, NASA report, interchange NCA2-OR745-716
Macphie, R. H., & Bracewell, R. N. 1979, Proc. SPIE, 172, 271
Marcy, G. W., & Butler, R. P. 1996, ApJ, 464, L147
Mariotti, J.-M., Coude de Foresto, V., Perrin, G., Zhao, P., & Lena, P. 1995, preprint
Mayor, M., & Queroz, D. 1995, Nature, 358, 355
Moseley, H. 1995, private communication
Owen, T. 1980, in Strategies for the Search for Life in the Universe, ed. M. D. Papagiannis (Dordrecht: Reidel), 177
Ryle, M., & Neville, A. C. 1962, MNRAS, 125, 39
Shao, M. 1996, http:/huey.jpl.nasa.gov:80/sim/
Shao, M., & Colavita, M. M. 1992, ARA&A, 30, 457
Thompson, R. A. 1962, in ASP Conf. Ser. Vol. 6, Synthesis imaging in Radio Astronomy, ed. C. A. Perley, F. R. Schwab, & A. H. Bridle (San Francisco: ASP), 34
Werner, M. W., & Franson, J. 1995, Proc. SPIE, 2475, 418
Woolf, N., & Angel, J. R. P. 1995, in OSA Technical Digest Series 23, Adaptive Optics (Washington, DC: Optical Society of America)